Indonesian Journal of Chemical Research

http://ojs3.unpatti.ac.id/index.php/ijcr Indo. J. Chem. Res., 14 (1), 53-60, 2026

Morphological Study and Characterization of Chitosan/Graphene Quantum Dots/TiO_2 Composite Film as a Modified Electrode Material

Astri Anjelina Nasution[1*], Irwana Nainggolan[2], Andriayani[2], Nessa Gina Sonia[1]

[1] Postgraduate School, Department of Chemistry, Faculty of Mathematics and Natural Sciences, Universitas Sumatera Utara, Jl. Bioteknologi No. 1, Medan, 20155, Indonesia

[2] Department of Chemistry, Faculty of Mathematics and Natural Sciences, Universitas Sumatera Utara, Jl. Bioteknologi No. 1, Medan, 20155, Indonesia

[*]*Corresponding Author: irwana@usu.ac.id*

Received: December 2025
Received in revised:April 2026
Accepted: May 2025
Available online: May 2026

Abstract

This study investigates the morphological and structural characteristics of chitosan/graphene quantum dots/titanium dioxide (CS/GQDs/TiO_2) composite films with TiO_2 concentrations of 50–250 mg/L as coating materials for modified working electrodes. The films were prepared using ionic gelation and stirring methods. Characterization was performed using Fourier Transform Infrared Spectroscopy (FTIR), X-Ray Diffraction (XRD), and Scanning Electron Microscopy (SEM). FTIR analysis confirmed hydrogen bonding and coordination interactions among chitosan, GQDs, and TiO_2 through the shift of –OH/–NH_2 bands and the appearance of Ti–O–Ti and C–O–Ti bands. XRD analysis showed an increase in crystallinity from 20.82% to 41.35%, indicating improved structural ordering after TiO_2 incorporation. SEM observations revealed morphological transformation from the rough surface of pure chitosan to a more compact and homogeneous structure at moderate TiO_2 concentrations, while agglomeration appeared at higher concentrations. These results demonstrate that the incorporation of GQDs and TiO_2 enhances the structural stability and morphology of the chitosan matrix, making the composite promising for electrochemical electrode coating applications.

Keywords: Chitosan, GQDs, TiO_2, FTIR, XRD, SEM

INTRODUCTION

Electrochemical sensors are becoming widely recognized for their capacity to quickly, selectively, and sensitively identify a diverse array of chemical and biological substances. These sensors are widely applied in medical diagnostics, environmental assessment, food quality evaluation, and various biomedical applications due to their desirable properties, such as cost-effectiveness and facile integration into miniaturized analytical systems (Baranwal et al., 2022). The performance of electrochemical sensors is largely determined by the properties of the electrode materials, such as high electrical conductivity, large active surface area, and excellent electrochemical activity, which are essential for efficient electron transfer and sensitive analyte detection (Obeid et al., 2025). Numerous types of nanostructured materials have been extensively explored for electrochemical applications. This category of materials includes carbon-based nanomaterials such as graphene and its related nanostructures, metal nanoparticles, including gold and platinum, metal oxide nanoparticles such as TiO_2 and MnO_2, as well as various types of nanopolymers (Zhou et al., 2023). Chitosan, a naturally occurring polymer derived from the deacetylation of chitin, has attracted considerable interest in the area of electrochemical sensing applications. Its attractiveness stems from a unique set of remarkable characteristics, particularly its superior biocompatibility, biodegradability, and large surface area, all of which collectively enhance the performance and effectiveness of electrochemical sensors (Prabhu et al., 2022). Chitosan contains two main reactive functional groups, namely amino (-NH_2) and hydroxyl (-OH) groups located at primary and secondary carbon positions (Zouaoui et al., 2020). The amino groups in chitosan create a hydrophilic environment that supports biomolecular interactions and can be protonated under acidic conditions, making it a cationic polyelectrolyte. This positive charge enables chitosan to interact with anionic molecules, thereby enhancing analyte adsorption and current response in electrochemical applications (Annu & Raja, 2020;

Bocchetta et al., 2024). The ability of chitosan to undergo various chemical functionalizations and structural modifications renders it a highly suitable candidate for electrochemical sensor fabrication. Incorporating chitosan with nanomaterials can improve the sensitivity, selectivity, and stability of electrochemical sensors; for example, graphene quantum dots (GQDs) can facilitate direct electron transfer (Mansuriya & Altintas, 2020). Meanwhile, combining chitosan with metal oxides enhances its mechanical, optical, electronic, and catalytic properties. This multifunctional combination-structural stability, selective adsorption, ease of modification, and synergy with other materials-establishes chitosan as a versatile material for advancing innovation in electrochemical sensor technology (Annu & Raja, 2020).

Among various carbon-based nanomaterials, graphene quantum dots (GQDs) have attracted significant attention because of their excellent electrical conductivity, high surface area, chemical stability, and superior electron transfer capability. These properties make GQDs highly promising for electrochemical sensing applications (Jiménez-López et al., 2020; Mahajan & Patil, 2022). Numerous studies have explored the use of GQDs as sensing materials. For instance, Arumugasamy et al (2020) successfully combined GQDs with functionalized multi-walled carbon nanotubes (MWCNTs) for dopamine detection, demonstrating excellent electrocatalytic activity toward dopamine oxidation (Arumugasamy et al., 2020). In the environmental field, Tanwar et al (2023) employed GQDs modified glassy carbon electrodes for the detection of the pesticide residue malathion, achieving high sensitivity and stability (Tanwar et al., 2023).

Various metal oxide nanomaterials have been widely explored for electrochemical sensor applications due to their favorable physicochemical properties, including low cost, ease of synthesis, biocompatibility, and catalytic activity (Liu et al., 2022). Among them, titanium dioxide (TiO_2) has attracted considerable attention because of its semiconductor characteristics, high surface reactivity, large specific surface area, and excellent electrocatalytic performance. These properties enable TiO_2 to enhance electron transfer efficiency and improve sensor sensitivity toward various target analytes. Several studies have demonstrated the potential of TiO_2-based materials in electrochemical sensing applications. For example, Ohse et al. (2024) developed a TiO_2-x/CuxO nanostructured electrochemical sensor for glyphosate detection in water samples, exhibiting high sensitivity and stability (Ohse et al., 2024). In addition, Thakur et al. (2025) reported the successful fabrication of a TiO_2/polypyrrole-based electrochemical sensor for glucose detection with excellent analytical performance and reliability (Thakur et al., 2025).

The combination of GQDs and TiO_2 within the chitosan matrix produces a synergistic effect. GQDs enhance electrical conductivity and facilitate faster electron transfer, while TiO_2 increases the active surface area and provides catalytic sites. This integration overcomes the limitations of chitosan as a single material, thereby enhancing the analytical responsiveness and discrimination capability of electrochemical sensors toward target analytes.

Previous studies have mainly focused on the application of chitosan-based nanocomposites as electrochemical sensors, particularly emphasizing sensing performance and analytical sensitivity. However, limited studies have specifically investigated the modification process and comprehensive characterization of chitosan/GQDs/TiO_2 composite films before their electrochemical application. As a result, the effects of GQDs and TiO_2 incorporation on the structural, crystalline, and morphological properties of the composite matrix have not been fully understood. Therefore, this study focuses on the preparation and characterization of chitosan/GQDs/TiO_2 composite films with different TiO_2 concentrations using ionic gelation and stirring methods. The novelty of this work lies in the systematic investigation of the structural and morphological evolution of the composite film as a potential coating material for modified working electrodes.

In this study, the three components were integrated using ionic gelation and stirring methods, which are widely employed because of their simple procedures, controllable parameters, and ability to produce homogeneous composite systems (Nainggolan, Saisa, et al., 2024). The prepared chitosan/GQDs/TiO_2 composite films were characterized using Fourier Transform Infrared Spectroscopy (FTIR), X-Ray Diffraction (XRD), and Scanning Electron Microscopy (SEM).

METHODOLOGY

Materials and Instrumentals

The materials used in this study included commercially available medium molecular weight chitosan (CS) (Sigma-Aldrich), graphene quantum dots (GQDs) (ACS Materials), titanium dioxide (TiO_2)

(NRE), glacial acetic acid, anhydrous oxalic acid, and deionized water.

The instruments used in this study included an ultrasonic bath (GYYSON PULSATRON MKCSS Kerry), Fourier Transform Infrared Spectroscopy (FTIR, Perkin-Elmer UATR Spectrum Two), X-Ray Diffraction (XRD, Shimadzu MAXima_X XRD-7000), and Scanning Electron Microscopy coupled with Energy Dispersive X-ray Spectroscopy (SEM-EDX, JEOL JSM-6510LA). The prepared chitosan/GQDs/TiO_2 composite films were characterized using these instruments to evaluate their structural, crystalline, and morphological properties.

Chitosan/GQDs/TiO_2-based thin film preparation

The chitosan was dissolved in acetic acid to create the chitosan thin film. Gelation and stirring are two methods selected for the dissolution process because to their simplicity and the uniformity of outcomes. 1.5 g of chitosan was introduced into a beaker, followed by the addition of 100 mL of 2% (v/v) acetic acid. The solution was then subjected to continuous stirring at a temperature range of 30-45 °C for a duration of 24 hours, ensuring a homogeneous mixture was achieved (Nainggolan, Martina et al., 2024).

Chitosan/GQDs/TiO_2 (CS/GQDs/ TiO_2) thin films were fabricated through multiple stages. A concentration of 250 mg/L of GQDs was mixed with varying concentrations of TiO_2 (50, 100, 150, 200, and 250 mg/L) in a 1:1 ratio under constant stirring at 200-300 rpm for 1 hour. Secondly, chitosan was blended with a GQDs/TiO_2 solution at a ratio of 2:1. The mixture was continuously stirred at 30-45 °C for 24 hours until homogeneous, followed by an ultrasonication process for 1 hour. The characterization of each treatment was conducted using FTIR, XRD, and SEM techniques.

Data Analysis

Fourier Transform Infrared Spectroscopy (FTIR) was employed to characterize the CS/GQDs/TiO_2 thin films and to determine the functional groups present in the composite materials. X-ray diffraction (XRD) analysis was carried out to examine the crystalline structure and phase arrangement of the composite material. Scanning Electron Microscopy (SEM) analysis was conducted to investigate the surface features and morphological changes of CS/GQDs/TiO_2 thin films (with TiO_2 concentrations ranging from 50 to 250 mg/L).

RESULTS AND DISCUSSION

Visual Appearance of Chitosan/GQDs/TiO_2 Composite Solutions

Chitosan, GQDs, and TiO_2 were first dissolved or dispersed in their respective solvents before composite preparation. The dissolution and mixing processes were carried out using ionic gelation, magnetic stirring, and ultrasonication methods to obtain homogeneous composite solutions.

Figure 1. Visual appearance of CS/GQDs/TiO_2 composite solutions with different TiO_2 concentrations before film formation

Figure 1 shows the visual appearance of CS/GQDs/TiO_2 composite solutions with different TiO_2 concentrations before film formation. As the TiO_2 concentration increased, the composite solutions became opaquer and more turbid, indicating increased particle incorporation within the chitosan matrix. At lower TiO_2 concentrations, the mixtures appeared relatively homogeneous, while slight aggregation became visible at higher concentrations.

Fourier Transform Infrared (FTIR) Analysis

The functional group analysis of the CS/GQDs/TiO_2 film was carried out using Fourier Transform Infrared Spectroscopy (FTIR). Each functional group in the CS/GQDs/TiO_2 film exhibits various wavenumbers based on its vibrational capabilities and energy absorption from the infrared spectrum. Fourier transform infrared (FTIR) examination employing Shimadzu IR Prestige-21 equipment was carried out throughout a wavenumber range of 500-4000 cm^{-1}. The samples analyzed included CS, CS/GQDs, and CS/GQDs/TiO_2 films. In the FTIR spectra, the presence of peaks or bands in the transmittance spectrum indicates the formation of specific chemical bonds within the tested samples.

Figure 2 shows the FTIR spectra of chitosan, chitosan/GQDs, and chitosan/GQDs/TiO_2 film. There are some specific bands related to functional groups in chitosan/GQDs and chitosan/GQDs/TiO_2 films that are also visible in chitosan film, such as the existence of intermolecular and intramolecular hydrogen bonding, which was discovered by peaks displayed at 3448.7 cm^{-1} and 3427.5 cm^{-1}.

Figure 2(a) shows that chitosan exhibits distinct absorption peaks, indicating the presence of its inherent functional groups. The large peak found at 3448.7 cm^{-1} corresponds to the overlapping stretching vibrations of –OH and $–NH_2$ groups. The absorption band at 2922.1 cm^{-1} is due to the C–H stretching vibrations of the aliphatic groups ($–CH_2–$) in chitosan. The peak at 1633.7 cm^{-1} represents the C=O stretching vibration of the –NHCO– group in primary amides (amide I), while the band showing at 1413.8 cm^{-1} is related to the N–H bending vibration of the amide bond (Hasanela et al., 2020; Patehkhor et al., 2021; Tanasale et al., 2018).

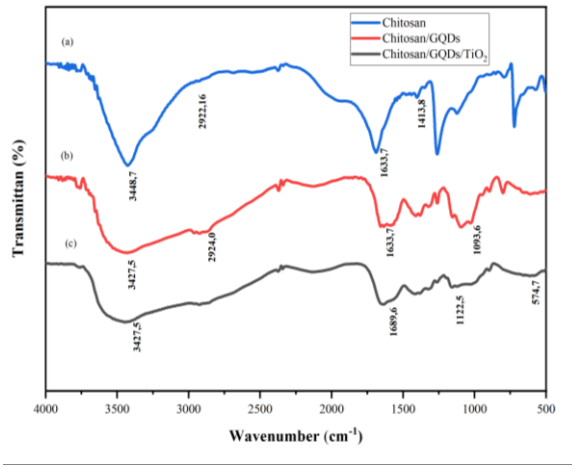

Figure 1. FTIR spectra of CS (a), CS/GQDs (b), and CS/GQDs/TiO_2 (c)

Figure 2(b) the chitosan/GQDs spectrum exhibited several characteristic bands, including an asymmetric stretching vibration of C-O-C at 1093.6 cm^{-1}, indicating an interaction between GQDs and the ether/hydroxyl groups of chitosan. Additionally, a slight shift of the -OH/$-NH_2$ stretching band to a lower wavenumber at 3427.5 cm^{-1} suggests the presence of a hydrogen bonding interaction between the chitosan -OH/$-NH_2$ groups and the oxygen-containing functional groups (C=O, COOH) of GQDs. The absorption band at 2924.0 cm^{-1} corresponds to the C-H stretching vibration. N-H bending vibration in chitosan film is observed at 1633.7 cm^{-1}, corresponding to the principal amine bonds (Tanwar et al., 2023).

The FTIR spectrum 2(c) of chitosan/GQDs/TiO_2 100 mg/L shows a distinct absorption band at 574.7 cm^{-1} corresponding to the characteristic stretching vibration of Ti-O-Ti, confirming the successful incorporation of TiO_2 into the composite. The band at 3427.5 cm^{-1} remains associated with -OH stretching, but its reduced intensity indicates that part of the -OH groups interact with the TiO_2 surface. The band at 1689.6 cm^{-1}, slightly shifted from 1633.7 cm^{-1}, suggests the formation of coordination interactions between the $-NH_2$ groups of CS and Ti^{4+} ions. Additionally, the band at 1122.5 cm^{-1} corresponds to the C-O-Ti stretching vibration, further confirming the formation of chemical bonds between chitosan/GQDs and TiO_2 (Alduwaib et al., 2024).

The observed shift in the -OH/$-NH_2$ peaks indicates the presence of hydrogen bonding and the formation of a coordination interaction of TiO_2 with chitosan and GQDs. The results obtained from the FTIR analysis are presented in Table 1.

Table 1. FTIR absorption bands and functional group assignments of CS, CS/GQDs, and CS/GQDs/TiO_2 composite films.

Material	Wavenumber (cm^{-1})	Functional group
CS	3448.7	-OH/$-NH_2$ stretching
	2922.1	C-H stretching
	1633.7	C=O stretching
	1413.8	N-H bending
CS/ GQDs	3427.5	-OH/$-NH_2$ stretching
	2924.0	C-H stretching
	1633.7	N-H bending
	1093.6	C-O-C stretching
CS/ GQDs/ TiO_2	3427.5	-OH/$-NH_2$ stretching
	1689.6	C=O stretching
	1122.5	C–O–Ti stretching
	574.7	Ti–O–Ti stretching

X-Ray Diffraction (XRD) Analysis

The crystal characterization of the chitosan/GQDs and chitosan/GQDs/TiO_2 film was carried out using the X-ray Diffraction (XRD) method within a range of 10^0-90^0. The XRD spectrum shows the relationship between the scattering angle (2θ) and the peak intensity. The diffraction peaks of the chitosan/GQDs and chitosan/GQDs/TiO_2 film were compared to identify the crystalline structure formed. The XRD characterization result of the chitosan/GQDs and chitosan/GQDs/TiO_2 films is shown in Figure 3.

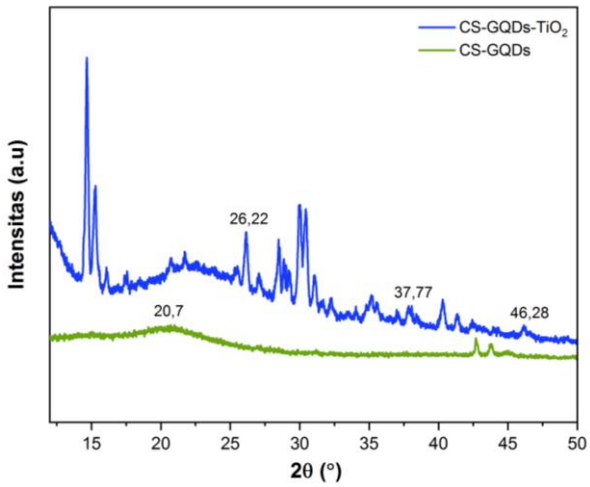

Figure 2. X-ray Diffractogram Curve of CS/GQDs and CS/GQDs/TiO_2

The X-ray diffraction pattern of the chitosan/GQDs exhibits two peaks at 20.7° and 23.3°, which can be attributed to the hydrated crystalline structure of chitosan, characterized by hydrogen bonding between amino and hydroxyl groups (Rahmatian et al., 2024). These features also indicate the amorphous nature of the chitosan/GQDs structure (Esmaeilzadeh et al., 2020). The XRD pattern of chitosan/GQDs/TiO_2 shows distinct reflections at 26.22°, 37.77°, and 46.28°, corresponding to GQDs/TiO_2 phases (Norouzi et al., 2022; Utomo & Wihadi, 2022). After adding TiO_2, there is a noticeable peak shift. This is because the chitosan crystalline domains are only partially broken up by gelatinization and strong hydrogen bonding interactions between the chitosan and TiO_2 components (Liu et al., 2022). The crystallinity index went up from 20.82% for chitosan/GQDs to 41.35% for chitosan/GQDs/TiO_2. This increase in crystallinity is probably because Ti atoms from TiO_2 and N atoms from chitosan form coordination bonds. These bonds make the matrix network stronger through chemical–physical interactions, which in turn encourage the rearrangement of polymer chains into a more ordered structure.

Scanning Electron Microscopy (SEM) Analysis

Observation of the surface morphology of the chitosan, chitosan/GQDs, and chitosan/GQDs/TiO_2 thin film was carried out using scanning electron microscopy (SEM), SEM-EDX JEOL JSM-6510LA. The result of chitosan, chitosan/GQDs, and chitosan/GQDs/TiO_2 (with TiO_2 concentration variations ranging from 50 to 20 mg/L**).** Preparation of matrices, which were fabricated into thin film layers, was conducted, followed by SEM measurements to observe the morphology of the thin film layers, as illustrated in Figure 3.

Based on the SEM analysis, the surface morphology of pure chitosan, shown in Figure 4(a), exhibited a relatively rough and irregular surface with slight perforations and band-like structures. These morphological features are attributed to the self-aggregation behavior of chitosan molecules during film formation. In Figure 4(b), chitosan/GQDs show a more organized and even structure that looks like solid rods or cylinders. This is because graphene is present in the matrix (Tohamy et al., 2023). The incomplete interaction between chitosan and GQDs results in the production of rod-shaped (nanorod) structures.

The SEM image of chitosan/GQDs/TiO_2 with a TiO_2 concentration of 50 mg/L, presented in Figure 4(c), revealed a compact and well-organized fibrous or lamellar structure with a relatively smooth and uniform surface (Liu et al., 2022). The surface appears smooth and generally uniform. In Figure 4(d), chitosan/GQDs/TiO_2 100 mg/L, the surface structure becomes denser and more homogeneous, with a noticeable decrease in porosity. Fine granular features begin to appear, indicating an increase in particle density.

At a TiO_2 concentration of 150 mg/L (Figure 4(e)), the composite film exhibited a compact fibrous and interconnected network-like morphology. This structure is likely associated with the formation of a carbon network layer induced by TiO_2 incorporation (Hammi et al., 2021). Furthermore, the sample containing 200 mg/L TiO_2 (Figure 4(f)) displayed a denser morphology with fewer fibrous features and more uniformly distributed particles compared to the 150 mg/L sample.

In contrast, the composite film containing 250 mg/L TiO_2 (Figure 4(g)) exhibited a rough, cracked, and wavy surface morphology accompanied by significant particle agglomeration. At higher TiO_2 concentrations, nanoparticles tend to aggregate due to increased particle–particle interactions, resulting in non-uniform surface structures (Patehkhor et al., 2021). This observation is consistent with the findings of Moeen et al. (2022), which reported that increasing TiO_2 concentration led to significant particle agglomeration and reduced surface uniformity within the composite structure (Moeen et al., 2022).

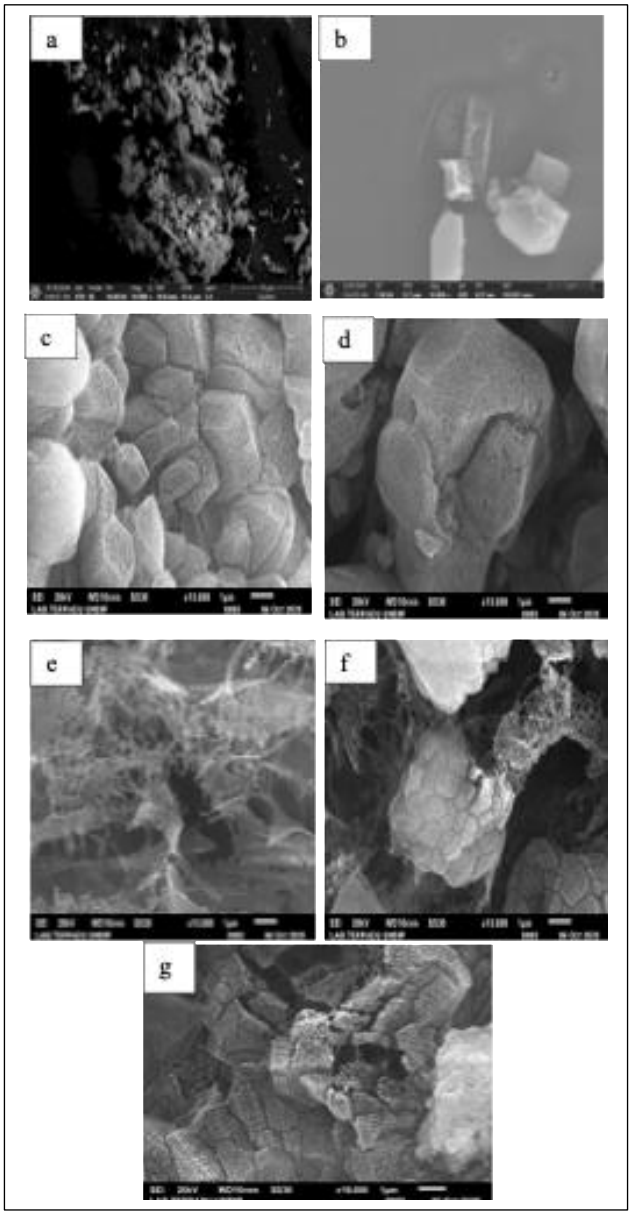

Figure 3. SEM micrographs of CS (a), CS/GQDs (b), CS/GQDs/TiO_2 50 mg/L (c), CS/GQDs/TiO_2 100 mg/L (d), CS/GQDs/TiO_2 150 mg/L (e), CS/GQDs/TiO_2 200 mg/L (f), and CS/GQDs/TiO_2 250 mg/L (g).

CONCLUSION

The results of this study demonstrated that the chitosan/GQDs/TiO_2 composite films were effectively prepared using ionic gelation and stirring methods, as confirmed by FTIR, XRD, and SEM analyses. The FTIR spectra indicated the formation of hydrogen bonding and coordination interactions among the composite components, evidenced by the shift of the –OH/–NH_2 absorption bands and the appearance of characteristic Ti–O–Ti and C–O–Ti bands at 574.7 cm^{-1} and 1122.5 cm^{-1}, respectively. XRD analysis revealed an increase in the crystallinity index from 20.82% to 41.35%, accompanied by the appearance of major diffraction peaks at 2θ = 26.22°, 37.77°, and 46.28°, indicating the successful incorporation of TiO_2 into the chitosan matrix. SEM observations further demonstrated morphological transformation from a rough chitosan surface to a more compact and homogeneous structure at a TiO_2 concentration of 100 mg/L, while excessive TiO_2 concentrations promoted particle agglomeration. Overall, the incorporation of GQDs and TiO_2 improved the structural and morphological properties of the chitosan matrix, suggesting its potential application as a coating material for modified working electrodes in electrochemical systems.

ACKNOWLEDGMENT

The authors gratefully acknowledge the financial support provided by the Agency for Agricultural Extension and Human Resource Development, Ministry of Agriculture of Indonesia, for this research.

REFERENCES

Alduwaib, S. M., Salih, S. A., & Jalal Al-den Fakar, D. (2024). Synthesis and characterization of TiO2- Ag- chitosan nano-composites in order to surface modification and bone tissue engineering using dip coating method. *Journal of Theoretical and Applied Physics*, *18*(1).

Annu, & Raja, A. N. (2020). Recent development in chitosan-based electrochemical sensors and its sensing application. *International Journal of Biological Macromolecules*, *164*, 4231–4244.

Arumugasamy, S. K., Govindaraju, S., & Yun, K. (2020). Electrochemical sensor for detecting dopamine using graphene quantum dots incorporated with multiwall carbon nanotubes. *Applied Surface Science*, *508*, 145294.

Baranwal, J., Barse, B., Gatto, G., Broncova, G., & Kumar, A. (2022). Electrochemical Sensors and Their Applications: A Review. *Chemosensors*, *10*(9).

Bocchetta, P., Othman, A., Gupta, M., Andriani, G., Martin, P., Kumar, Y., … Javed, M. S. (2024). Chitosan in electrochemical (bio)sensors: Nanostructuring and methods of synthesis. *European Polymer Journal*, *213*, 113092.

Esmaeilzadeh, M., Sadjadi, S., & Salehi, Z. (2020). Pd immobilized on hybrid of magnetic graphene quantum dots and cyclodextrin decorated chitosan: An efficient hydrogenation catalyst.

International Journal of Biological Macromolecules, *150*, 441–448.

Hammi, N., Marcotte, N., Marinova, M., Draoui, K., Royer, S., & Kadib, A. E. (2021). Nanostructured metal oxide@carbon dots through sequential chitosan templating and carbonisation route. *Carbohydrate Polymer Technologies and Applications*, *2*, 100043.

Hasanela, N., Tanasale, M. F. J. D. P., & Tehubijuluw, H. (2020). Characterization of Chitosan Biopolymers as Result of Deacetylation of Rajungan Crab Waste (Portunus sanginolentus) using NaBH4 in NaOH. *Indonesian Journal of Chemical Research*, *8*(1).

Jiménez-López, J., Llorent-Martínez, E. J., Ortega-Barrales, P., & Ruiz-Medina, A. (2020). Graphene quantum dots-silver nanoparticles as a novel sensitive and selective luminescence probe for the detection of glyphosate in food samples. *Talanta*, *207*, 120344.

Liu, Q., Xu, R., Mu, D., Tan, G., Gao, H., Li, N., … Wu, F. (2022). Progress in electrolyte and interface of hard carbon and graphite anode for sodium-ion battery. *Carbon Energy*, *4*(3), 458–479.

Mahajan, M. R., & Patil, P. O. (2022). Design of zero-dimensional graphene quantum dots based nanostructures for the detection of organophosphorus pesticides in food and water: A review. *Inorganic Chemistry Communications*, *144*, 109883.

Mansuriya, B. D., & Altintas, Z. (2020). Applications of Graphene Quantum Dots in Biomedical Sensors. *Sensors*, *20*(4).

Moeen, S., Ikram, M., Haider, A., Haider, J., Ul-Hamid, A., Nabgan, W., … Shahzadi, I. (2022). Comparative Study of Sonophotocatalytic, Photocatalytic, and Catalytic Activities of Magnesium and Chitosan-Doped Tin Oxide Quantum Dots. *ACS Omega*, *7*(50), 46428–46439.

Nainggolan, I., Martina, S. J., Alva, S., Li, B., Nasution, T. I., Sembiring, A., … Asrosa, R. (2024). Sensitivity of chitosan/reduced graphene oxide/manganese dioxide modified electrodes for cholesterol detection using cyclic voltammetry. *South African Journal of Chemical Engineering*, *48*, 329–336.

Nainggolan, I., Saisa, Agusnar, H., Alfian, Z., Alva, S., Nasution, T. I., Sembiring, A. (2024). Sensitivity of Chitosan Film Based Electrode Modified with Reduced Graphene Oxide (rGO) for Formaldehyte Detection Using Cyclic Voltammetry. *South African Journal of Chemical Engineering*, *48*, 184–193.

Norouzi, F., Pourmadadi, M., Yazdian, F., Khoshmaram, K., Mohammadnejad, J., Sanati, M. H., … Baino, F. (2022). PVA-Based Nanofibers Containing Chitosan Modified with Graphene Oxide and Carbon Quantum Dot-Doped TiO2 Enhance Wound Healing in a Rat Model. *Journal of Functional Biomaterials*, *13*(4).

Obeid, P. J., Sari-Chmayssem, N., Yammine, P., Homsi, D., El-Nakat, H., Matar, Z., … Chmayssem, A. (2025). Designs and Materials of Electrodes for Electrochemical Sensors. *ChemElectroChem*, *12*(19), e202500230.

Ohse, S. T., Morais, A., Felsner, M. L., Galli, A., & Sikora, M. de S. (2024). Nanostructured TiO2-X/CuXO-based electrochemical sensor for ultra-sensitive glyphosate detection in real water samples. *Microchemical Journal*, *205*, 111316.

Patehkhor, H. A., Fattahi, M., & Khosravi-Nikou, M. (2021). Synthesis and characterization of ternary chitosan–TiO2–ZnO over graphene for photocatalytic degradation of tetracycline from pharmaceutical wastewater. *Scientific Reports*, *11*(1), 24177.

Prabhu, A., Crapnell, R. D., Eersels, K., Grinsven, B. van, Kunhiraman, A. K., Singla, P., … Peeters, M. (2022). Reviewing the use of chitosan and polydopamine for electrochemical sensing. *Current Opinion in Electrochemistry*, *32*, 100885.

Rahmatian, N., Abbasi, S., Abbasi, N., & Yaraki, M. T. (2024). Green-synthesized chitosan-carbon dot nanocomposite as turn-on aptasensor for detection and quantification of Leishmania infantum parasite. *International Journal of Biological Macromolecules*, *270*, 132483.

Tanasale, M. F. J. D. P., Bandjar, A., & Sewit, N. (2018). Isolation Of Chitosan From Straw Mushroom (Vollvariella volvaceae) Hood And Its Application As Lead (Pb) Metal Absorbent. *Indonesian Journal of Chemical Research*, *6*(1), 44–50.

Tanwar, S., Sharma, A., & Mathur, D. (2023). A graphene quantum dots–glassy carbon electrode-based electrochemical sensor for monitoring malathion. *Beilstein Journal of Nanotechnology*, *14*, 701–710.

Thakur, A., Pal, S., Sharma, U., Sharma, A., Choudhary, M., Joshi, M. C., … Shukla, S. K.

(2025). Advanced TiO2-polypyrrole nanostructures enhance glucose detection accuracy with cutting-edge non-enzymatic electrochemical capabilities. *Chemical Physics Impact*, *10*, 100818.

Tohamy, H.-A. S., Fathy, N. A., El-Sakhawy, M., & Kamel, S. (2023). Boosting the adsorption capacity and photocatalytic activity of activated carbon by graphene quantum dots and titanium dioxide. *Diamond and Related Materials*, *132*, 109640.

Utomo, A. D. C., & Wihadi, Muh. N. K. (2022). Preparation of ZnO/TiO2 Nanocomposite Sensitized Mangosteen Rind (Garcinia mangostana L) Dye for Light Harvesting Efficiency in Solar Cell. *Indonesian Journal of Chemical Research*, *10*(2), 68–73.

Zhou, C., Feng, J., Tian, Y., Wu, Y., He, Q., Li, G., & Liu, J. (2023). Non-enzymatic electrochemical sensors based on nanomaterials for detection of organophosphorus pesticide residues. *Environ. Sci.: Adv.*, *2*(7), 933–956.

Zouaoui, F., Bourouina-Bacha, S., Bourouina, M., Jaffrezic-Renault, N., Zine, N., & Errachid, A. (2020). Electrochemical sensors based on molecularly imprinted chitosan: A review. *TrAC Trends in Analytical Chemistry*, *130*, 115982.